



**Ionic gelation encapsulation of sesame oil with sodium alginate-nopal mucilage blends:
Encapsulation efficiency and oxidative stability**

**Encapsulación por gelación iónica de aceite de sésamo con mezclas de alginato de
sodio-mucílago de nopal: Eficiencia de encapsulación y estabilidad oxidativa**

S.K. Velázquez-Gutiérrez¹, E. Alpizar-Reyes¹, J. Cruz-Olivares¹, J.F. Barrera-Pichardo¹, M.E. Rodríguez-Huezo²,
C. Pérez-Alonso^{1*}

¹Departamento de Ingeniería Química, Facultad de Química, Universidad Autónoma del Estado de México, Paseo Colón esq.
Paseo Tollocan s/n, Col. Residencial Colón, C.P. 50120, Toluca, Estado de México, México.

²Departamento de Ingeniería Química y Bioquímica, Tecnológico de Estudios Superiores de Ecatepec, Av. Tecnológico s/n esq.
Av. Central, Col. Valle de Anáhuac, Ecatepec, C.P. 55210, Estado de México, México.

Received: April 29, 2020; Accepted: June 25, 2020

Abstract

Hydrogel beads were formed by ionic gelation between sodium alginate-nopal mucilage (SA-NM) for enhancing the encapsulation efficiency and oxidative stability of sesame oil (SO). SA-NM blends (2% w/v) were used 1:1 and 1:1.5 (w/w) ratios. Ionic gelation was induced by dripping the SO-SA-NM homogenized dispersions with the help of a syringe into CaCl₂ (2.5% w/v) solution with continuous stirring. The resulting beads were oven-dried and stored under controlled temperature conditions. The hydrogel beads were evaluated for size and shape, and for SO encapsulation efficiency, oxidative stability, and release kinetics. Results were compared with hydrogel beads made with only SA (2% w/v). The SA beads had a regular spherical shape with a mean size of ~2.19 mm, while the SA-NM hydrogels beads had an irregular semi-spherical shape with a significant smaller (~2.06-2.10 mm) size. SA-NM hydrogel beads displayed higher encapsulation efficiency (> 75.44%) than SA beads (63.48%), and provided better protection to SO against oxidation during storage than the SA beads and free SO oil. Oxidation kinetics were of zero-order in all cases. The release kinetics of SO was diffusion controlled and was significantly slower for SA-NM than for SA beads. Our results indicate that SA-NM mixtures may be considered as potential additives for food industry applications.

Keywords: nopal mucilage, sodium alginate, ionic gelation, sesame oil, oxidative stability, encapsulation efficiency.

Resumen

Se formaron perlas de hidrogel por gelación iónica entre alginato de sodio - mucílago de nopal (SA - NM) para mejorar la eficiencia de encapsulación y la estabilidad oxidativa del aceite de sésamo (SO). Las mezclas SA - NM (2% w/v) se usaron en relaciones peso de 1:1 y 1:1.5 (w/w) a una concentración de 2% (w/v). La gelación iónica se indujo goteando las dispersiones homogeneizadas de SO - SA - NM con la ayuda de una jeringa en una solución de CaCl₂ (2.5% p/v) bajo agitación continua para inducir la gelación iónica. Las perlas resultantes se secaron en un horno de convección forzada y se almacenaron en condiciones controladas de temperatura. El tamaño y forma de las perlas de hidrogel se evaluaron, así como la eficiencia de encapsulación, la estabilidad oxidativa y la cinética de liberación de SO. Los resultados se compararon con perlas de hidrogel hechas con solo SA (2% w/v). Las perlas de hidrogel de SA presentaron una forma esférica regular de ~2.19 mm de tamaño promedio, mientras que las perlas de hidrogel de SA-NM tuvieron una forma semiesférica irregular con un tamaño promedio significativamente menor (~2.06-2.10 mm). Las perlas de los hidrogeles SA-NM mostraron una mayor eficiencia de encapsulación (> 75.44%) que las perlas de SA (63.48%), y también ofrecieron una mejor protección al SO contra la oxidación durante el almacenamiento en comparación con el aceite libre y las perlas de SA. Las cinéticas de oxidación fueron de orden cero. La cinética de liberación de SO fue controlada por difusión y fue más lenta para las perlas SA - NM que para las de SA. Nuestros resultados indican que mezclas de SA-NM pueden considerarse como aditivos potenciales para aplicaciones en la industria alimentaria.

Palabras clave: mucílago de nopal, alginato de sodio, gelación iónica, aceite de ajonjolí, estabilidad oxidativa, eficiencia de encapsulación.

* Corresponding author. E-mail: cpereza@uaemex.mx

<https://doi.org/10.24275/rmiq/Alim1655>

ISSN:1665-2738, issn-e: 2395-8472

1 Introduction

Among several distinct vegetable oils, the sesame oil (SO) (*Sesamum indicum* L.) is an important source of edible oil due to its high essential fatty acids (ω -3e6). The main compounds of the sesame oil are unsaturated fatty acids (UFA), ~47% of linoleic acid and ~37% of oleic acid (Corso *et al.*, 2010; Lee *et al.*, 2012). Both essential fatty acids are important in the human feed, because they offer health benefits. In the last years has been reported that the consumption of sesame oil influences in blood lipid profiles, increasing anti-inflammatory function, and exhibiting antimutagenic activity (Moreno-Santander *et al.*, 2020; Xu-Yan *et al.*, 2012). For this reason, numerous efforts have been made to fortify foods with ω -3e6 fatty acids to achieve a balanced intake. Unsaturated essential fatty acids in sesame oil are chemically unstable in presence of oxygen, light, moisture and heat. One of the major disadvantages in the incorporation of oils rich in ω -3e6 into food formulation is their high susceptibility to lipid oxidation (Shahidi & Zhong, 2005; Alpizar-Reyes *et al.*, 2020). The oxidation of lipids not only decreases their nutritional value but also results in the formation of toxic products as well as off-flavor and taste. Thus, these oils must be protected to make them more stable during handling, processing and storage (Plazola-Jacinto *et al.*, 2019; Pereyra-Castro *et al.*, 2019; Hernández-Centeno *et al.*, 2020). Stability of sesame oil can be enhanced through encapsulation process. Encapsulation of essential fatty acids was carried out using spray-drying (Fuentes-Ortega *et al.*, 2017), simple and complex coacervation (Timilsena *et al.*, 2019), and supercritical fluid precipitation (Martín *et al.*, 2010) resulting in their successful incorporation in product formulations. The ionic gelation method is one of the simplest approaches for the encapsulation, protection, and delivery of oils and other active agents (Bannikova *et al.*, 2016). In this method, a biopolymer solution or emulsion containing the bioactive compound is injected into another ??hardening?? solution under conditions that promote biopolymer gelation. This procedure results in the formation of a hydrogel bead with the bioactive trapped inside. The nature of the hydrogel matrix surrounding the bioactive can be designed to improve its physical and chemical stability, as well as to control its delivery. Typically, hydrogel beads with a particle diameter greater than about 1 mm are prepared using a syringe with a needle or a pipette (Li *et al.*, 2011).

Hydrogel beads suitable for utilization in foods are usually constructed from food-grade biopolymers such as proteins and/or polysaccharides using a variety of approaches (Chen *et al.*, 2006; Shewan & Stokes, 2013; Joye & McClements, 2014). Sodium alginate (SA), a typical wall material used in ionic gelation, is an anionic biopolymer composed of randomly distributed units of α -guluronic and 1,4-linked β -D-mannuronic acid residues (Hosseini *et al.*, 2013). The common method of producing alginate nano or micro particles compromise an oily compound is emulsification, followed by crosslinking using calcium chloride and solvent evaporation. Nopal mucilage (NM) from *Opuntia ficus indica* (a member of the cactaceae family) is a mixture of acidic and neutral polysaccharides consisting of 24.6-42 % of arabinose; 21-40.1 % of galactose; 8-12.7 % of galacturonic acid; 7-13.1 % of rhamnose and 22-22.2 % of xylose, besides of glycoproteins (Sáenz *et al.*, 2004). The NM has been used as water retainer, food thickener, emulsifier (León-Martínez *et al.*, 2010), encapsulating agent of bioactive compounds (Medina-Torres *et al.*, 2013). Nopal mucilage have been mixed with different biopolymers such as κ -carrageenan in 80:20 ratio getting higher gel rigidity than the pure κ -carrageenan, besides nopal mucilage increased the elasticity on the final gels (Medina-Torres *et al.*, 2003). Nopal mucilage mixed with sorghum starch resulted in an enhanced gel structure respect to starch gel control (Rivera-Corona *et al.*, 2014). Therefore, the method of ionic gelation can be a competitive alternative to the conventional encapsulation techniques most used (spray drying, freeze drying, complex coacervation, etc.) encapsulation of vegetable oils thermolabile as is the case of the sesame oil. The aim of this work was to develop hydrogel beads mixing nopal mucilage as wall material component so that it helps to improve the encapsulation efficiency and oxidative stability of sesame oil encapsulated with sodium alginate by the ionic gelation method.

2 Materials and methods

2.1 Materials

The sesame seeds were purchased from regional supermarket in Toluca City (Toluca, State of Mexico, Mexico). Nopal (*Opuntia ficus indica*) cladodes were obtained in a local market (Toluca, State of Mexico, Mexico) and were treated to eliminate spines and then

washed. Commercial sodium alginate (SA) was kindly supplied by FMC Health & Nutrition (Ciudad de México, México) (Protanal® RF 6650 Alginate). This biopolymer has a purity of 90%, a high molar mass sodium alginate with a high content of guluronic acid (65%) and a viscosity of between 400 and 600 mPas in a 1% solution at 20 °C, according to the supplier. All reagents were of analytical grade and were purchased from Sigma-Aldrich Química, S.A. de C.V. (Toluca, State of Mexico, Mexico). All the water used in the experiments was deionized.

2.2 Extraction of sesame oil (SO)

A Tamer hydraulic press (Model PT-20, Shanghai, China) fitted with a 40 cm long and 10 cm diameter plunger was used for cold pressing the sesame seeds for obtaining the sesame oil. Maximum pressure applied by the piston was 8.8×10^8 N/m² to the piston, at room temperature (~20 °C). Trace amounts of seed were removed from sesame oil using a cloth filter, and filtered sesame oil was stored in amber bottles at a temperature of ~5 °C until required (Fuentes-Ortega *et al.*, 2017).

2.3 Nopal mucilage (NM) extraction

Nopal mucilage was extracted from the cladodes following Cortés-Camargo *et al.* (2018) procedure with slight modifications. Briefly, nopal cladodes were cut into small slices with a contact area and thickness of 36 cm² and 2±0.2 mm respectively. The slices were weighed and put into a 3.5 L stainless steel container and distilled water was added in 1:2.5 nopal-water ratio. The nopal-water mixture was kept under agitation at 86 °C for 2.5 h, then the aqueous phase was separated from solid mass by decantation, and was filtered using a metallic sieve (No. 100). The filtered aqueous dispersion was spread on a drying tray and dried at 65 °C for 4 h in an air convection heat oven HCX II model (San-son plus, State of Mexico, Mexico). The dried nopal mucilage was standardized in size using a 40 mesh screen (420 μm).

2.4 Preparation of dispersions and hydrogel beads

Stock aqueous dispersions of SA (2% w/v) and NM (2% w/v) were prepared with deionized water and kept overnight in a shaking at 20 °C to warrant a full hydration of the biopolymers. The wall materials used were pure SA and SA-NM blends (mass ratios of 1:1

and 1:1.5). Then, 10 grams of sesame oil were added per each 100 grams of biopolymer stock aqueous dispersions under continuous agitation with an Ultra-Turrax T50 homogenizer (IKA®-Werke Works Inc., Wilmington, NC, USA) at 6400 rpm during 10 min (Rodea-González *et al.*, 2012). Subsequently, a sample of each homogenized dispersion was extracted in a 10 mL syringe attached with a 0.70 mm tip diameter of needle (22 gauge) and dripped into an aqueous solution of 100 mL of calcium chloride (2.5% w/v) contained in a beaker with a stirring of 250 rpm by means of a mechanical stirrer to prevent the agglomeration of beads. The tip of the needle was fixed at 30 cm above the surface of the crosslinking solution. The dropping rate was fixed at 20 drops per minute. The gelling solution (SO - SA - NM / CaCl₂ solution) was stirred for 60 min at 20 °C to complete gelation and produce beads.

The gelling solution was then washed with deionized water and filtered through a 355 μm mesh and subsequently dried in an oven at 45 °C for 24 h. Finally, the hydrogel beads were stored in amber flasks until later use.

2.5 Hydrogel beads morphology study

The optical microscopy images of the internal structure, size and shape of the hydrogel beads were obtained in an image analyzer system conformed for an optical microscope (MOTIC BA-400, Xiamen microscope, Shanghai, China), a digital camera and the software (MOTIC IMAGES PLUS 3.0 software, Shanghai, China). Selected micrographs at 10× were used for illustration. The beads were carefully cut in half with the help of a scalpel, in order to obtain internal faces of the beads; subsequently the samples were placed on a slide, covered with a coverslip and examined under microscope.

Sphericity factor (*SF*) was used to indicate the roundness of the beads, as described by Chan (2011), where a value equal to zero indicates a perfect sphere and higher values indicate a greater degree of shape distortion. *SF* was calculated according to Eq. (1):

$$SF = \frac{D_{max} - D_{per}}{D_{max} + D_{per}} \quad (1)$$

where D_{max} is the maximum diameter passing through the bead centroid (mm) and D_{per} is the perpendicular diameter to D_{max} passing through the bead centroid (mm). All samples were assayed in triplicate to determine the mean and standard error. The bead size

and shape were determined based on the measurement of 50 beads per sample.

2.6 Characterization of the hydrogel beads

The characterization of the hydrogel beads is based on the evaluation of the performance established by the yield (Y%), encapsulation efficiency (EE%) and payload (%), these factors determine the quality of the encapsulation process.

2.6.1 Encapsulation process yield (Y%)

The yield is the rate between the number of beads obtained and the amount of the SO-SA-NM dispersion used in the encapsulation process. The encapsulation process yield was calculated by using the following equation:

$$Y(\%) = \frac{M_b}{M_{em}} \times 100 \quad (2)$$

where:

M_b =Weight of hydrogel beads obtained.

M_{em} =Weight of SO-SA-NM dispersion used.

2.6.2 Encapsulation efficiency (EE%)

The amount of surface oil in the hydrogel beads was measured as the extracted oil after stirring at 250 rpm by means of a mechanical stirrer in n-hexane without disruption of beads structure among 60 s, assuming that this time was adequate in extracting the free oil from bead surface (Rodea-González *et al.*, 2012; Vasile *et al.*, 2016). Approximately 1 g of beads was shaken in a flask with 20 mL of n-hexane during 60 s. The supernatant was transferred to a previously weighted tube and the surface oil was determined by differences in weight after solvent evaporation under nitrogen atmosphere at room temperature (Vasile *et al.*, 2016).

Total oil of the hydrogel beads was determined using the method proposed by Rodea-González *et al.* (2012) with modifications. One gram of beads was placed into 20 mL of n-hexane and was sonicated (Sonics Vibra Cell VCX 130 PB, Sonics & Materials, Inc., Newtown, CT, USA) at 70% amplitude and frequency of 20 kHz for 10 min. Then the sesame oil was extracted with a Soxhlet extraction system during 6 h at room temperature. The solvent with the sesame oil was dried in a forced convection drying oven (Riossa, model E-51, Mexico City, Mexico) by solvent evaporation at 60-80 °C until constant weight was achieved. The weight of sesame oil collected after

extraction was taken as the content of total oil in the beads. The payload was calculated as follows:

$$\text{Payload (\%)} = \frac{O_{total}}{W_{beads}} \times 100 \quad (3)$$

Finally, the encapsulation efficiency was calculated from equation (4):

$$EE\% = \frac{(O_{total} - O_{surface})}{O_{total}} \times 100 \quad (4)$$

where total oil (O_{total}) is the sesame oil internal and surface content of hydrogel beads, while surface oil ($O_{surface}$) is the sesame oil corresponded to the un-encapsulated oil content found at the surface of the beads and W_{beads} is the weight of beads used.

2.7 Oxidative stability of encapsulated and free sesame oil

For sesame oil oxidation assessment, hydrogel beads and free sesame oil were stored at 25, 35, 45 °C, and stored during 21 days prior to achieve the equilibrium with a water activity of 0.329, 0.318 and 0.313, respectively. Beads and free oil were spread in pans of 3.5 cm of diameter (surface area of 9.6 cm²), and stored in sealed containers. Samples were not exposed to light during storage (Escalona-García *et al.*, 2016).

Lipid oxidation was evaluated during 8 weeks through the peroxide value (PV) expressed as milliequivalents of active oxygen per kilogram of oil (mEq/kg oil). The oil in the beads was extracted according to the method proposed by Bligh & Dyer (1959) with minor modifications. Briefly, the beads were milled in a mortar and washed with 5.7 mL of methanol, 2 mL of deionized water and 2.4 mL of chloroform. After homogenization, 3 mL of deionized water and 3.5 mL of chloroform were added. The mixture was transferred to a separate funnel. Upper phase containing oil in chloroform was separated and desorbed by solvent evaporation at room temperature under nitrogen flow until constant weight. Extracted oil was stored at -5 °C in sealed vials.

The peroxide value corresponding to encapsulated as well as free sesame oil was determined spectrophotometrically according to Shantha & Decker (1994) with light modifications. 0.2 mL of the oil extracted from the beads (or 0.2 g in the case of free oil) was added to 2.8 mL of a methanol/butanol (2:1 v/v) mixture. For color formation, 15 µL of an ammonium thiocyanate/iron (II) chloride solution was added. The sample was vortexed for 4 s, reacted

in the dark for exactly 5 min, and absorbance was measured at 510 nm in a Genesis 10 UV spectrometer (Thermo Scientific, Waltham, MA, USA). Sesame oil in hydrogel beads and free sesame oil samples were analyzed.

2.8 Kinetic analysis of lipid oxidation

As already mentioned, lipid oxidation involves many steps. However, in this work only the formation of hydroperoxides was analysed. In order to achieve this, the data of lipid peroxidation of encapsulated and free sesame oil stored at 25, 35 and 45 °C were fitted to zero-, first-, and second-order kinetics model, using Equations (5), (6), and (7), respectively (Levenspiel, 1999; Charoen *et al.*, 2015):

$$C_{HP} = -K_{HP}t + C_{HP_0} \quad (5)$$

$$\ln C_{HP} = \ln C_{HP_0} - K_{HP}t \quad (6)$$

$$1/C_{HP} = K_{HP}t + (1/C_{HP_0}) \quad (7)$$

where C_{HP_0} is the initial peroxide value at day 0 once the samples were conditioned at the a_w and temperature required; C_{HP} is the peroxide value after t (time) at a given temperature; K_{HP} is the hydroperoxide formation rate constant, which was obtained from the slope of a plot of lipid hydroperoxide *vs* time.

The effect of temperature on hydroperoxide formation was assessed using an Arrhenius relationship, which has demonstrated its applicability to describe the temperature dependence on the reaction rate (Pu & Sathivel, 2011). The apparent activation energy was obtained from Equation (8) (Fogler, 2006).

$$\ln K_{HP} = \left(-\frac{Ea}{RT} \right) + \ln A_{HP} \quad (8)$$

where K_{HP} is the apparent rate constant of hydroperoxide formation; Ea is the apparent activation energy; T is the absolute temperature (K); R is the universal gas constant (8.314 J/ mol K); and A_{HP} is the frequency factor.

2.9 Release kinetics of sesame oil extracted in hydrogel beads systems

Release kinetics of sesame oil extracted from beads were carried out at 25 °C and water activity of 0.329. A sample of each system of beads (1 g) was washed for 60 s with n-hexane to remove surface oil. Subsequently, 1 g of hydrogel beads from each system

was placed in 12 beakers containing 20 mL of n-hexane and it was slowly stirred, and the beads from the beakers were removed at intervals of 1, 5, 10, 15, 20, 25, 30, 40, 60, 90, 120 and 180 min by filtration. The supernatants of each beaker were placed in an oven at 35 °C to evaporate the solvent as well as the excess solvent in the beads. Finally, the release of the oil was quantified by difference in weight between the beads and the oil obtained from the removal of the solvent residue after drying in the oven.

2.10 Statistical analysis

Statistical analysis was performed in triplicate for each sample for all the tests, and data are shown as means \pm standard deviation. Data were analyzed using a one-way analysis of variance (ANOVA) and Tukey's test at a significance level $p \leq 0.05$ using Minitab version 16.0 software (Minitab Inc., State College, PA, USA).

3 Results and discussion

3.1 Morphology, size and shape of hydrogel beads

The light microscopy images (Figure 1a) of the SA beads show dry particles with spherical shape. After the drying process, the Ca^{2+} - alginate beads preserved their original sphericity with small surface irregularities. The preservation of the three-dimensional structure of beads after water loss may be attributed to the high content of G-blocks of guluronic acid. The G-blocks structure crosslinks with calcium, making possible the ionic gelation of an "egg box" like structure. While M-blocks cannot make similar linkages because of their "linear" structure (Ramos *et al.*, 2018). Therefore, the G-blocks content is one of the process variables that allows stronger structural networks in gel formation. On the other hand, SA-NM hydrogel beads (1: 1 and 1: 1.5 w / w) have less sphericity and irregular spheres shape than SA beads (Figures 1b, 1c). This is due to the weaker mechanical stability of the NM-calcium network compared to that from alginate-calcium. So that SA-NM hydrogel beads after the drying process leads to a slightly elongated sphere and less spherical shape than the SA beads.

In general, the dried hydrogel beads showed spherical shape and smooth surface, with some collapses and cracks observed in the alginate ones.

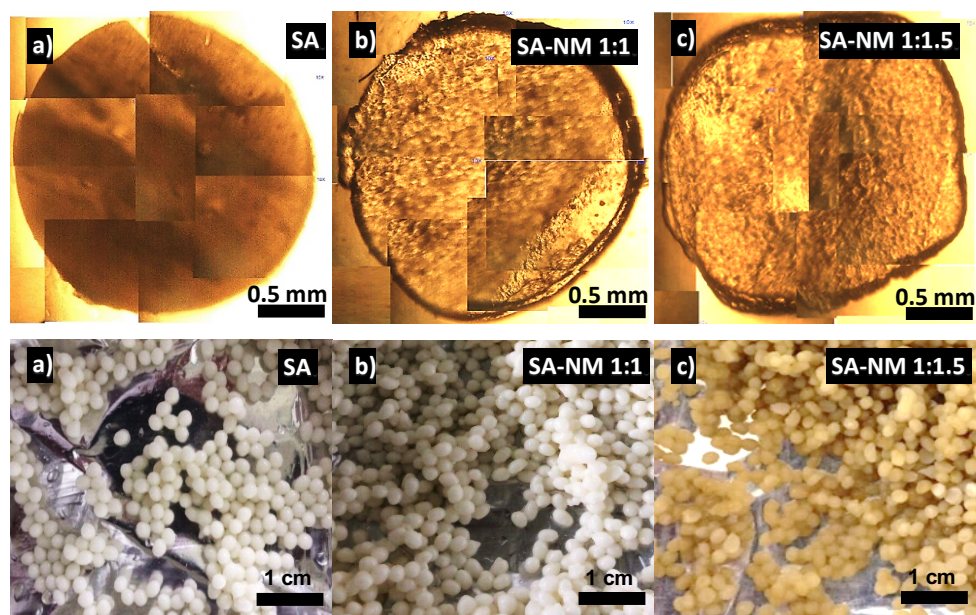


Figure 1. Optical microscopy images of internal surface and external aspect of the hydrogel beads.

Table 1. Characterization of the hydrogel beads.

	SA	SA-NM (1:1)	SA-NM (1:1.5)
Size (mm)	2.19± 0.13 ^a	2.06± 0.10 ^{a^c}	2.10± 0.06 ^{a^b}
SF (-)	0.049± 0.003 ^a	0.062± 0.002 ^b	0.065± 0.004 ^b
Yield (Y%)	72.50 ± 0.42 ^a	83.34 ± 0.51 ^b	91.67 ± 0.87 ^c
Surface oil (%)	7.83 ± 0.16 ^c	6.20 ± 0.09 ^b	5.48 ± 0.14 ^a
Encapsulation efficiency (EE%)	63.48 ± 0.35 ^a	75.44 ± 0.37 ^b	80.64 ± 0.51 ^c
Payload (%)	15.01 ± 0.07 ^a	25.24 ± 0.16 ^b	40.44 ± 0.14 ^c

Values are means ± standard error, of three replicates. Superscripts with different letters in same row indicate significant differences ($p \leq 0.05$).

The SA-NM hydrogel beads had heterogeneous surface morphologies and a wrinkled spongy shape. In the systems where the NM is incorporated as wall material is embedded in the gel matrix, acting as “structural support” and thus controlling fractures in the beads after drying, making the gel matrix more flexible.

According to Table 1, the size of the dried hydrogel beads fell in the range between 2.06 ± 0.10 mm and 2.19 ± 0.13 mm. The difference in size of the different types of hydrogel beads was relatively small and may be associated with the high water-holding capacity of NM in the formation of three-dimensional networks

of hydrogels. Spherical beads are more appreciated by the consumer and are easier to manipulate. As reported by Chan *et al.* (2011) the microparticles should have a $SF < 0.05$ to be considered spherical. SA hydrogel beads exhibited SF values of 0.05, while the SA-NM hydrogel had SF values slightly greater than 0.05. This can be explained by the differences in viscosity of the dispersions (data not reported) that can alter the fluidity during dripping, affecting the drop shape. During crosslinking with calcium, the shape of the bead tends to remain, but the effect on the form is not evident. For dried beads, the effect of oil content on the shape becomes noticeable (Benavides *et al.*, 2016).

3.2 Characterization of the hydrogel beads

The hydrogel beads obtained were evaluated according to the Yield (Y%), Encapsulation Efficiency (EE%) and Payload (%), of the encapsulation process, with the following results: Table 1 shows the results of the characterization of the hydrogel beads. All beads formulations presented high yield percentages for the encapsulation process of sesame oil ranging from 72 to 92%. The high yields obtained can be explained by the fact that there was no considerable loss of the dispersion during its transfer to the syringe, and in the same way during the dripping process through the syringe. Hydrogel beads showed a significant increase in yield percentage as the amount of nopal mucilage increased in SA-NM mixtures; this is possibly due to the complex interaction that occurs between both biopolymers with calcium ions, forming stronger and more robust cross-linked networks in the spherification process, compared to the interactions that form between SA and calcium ions.

Another critical parameter normally considered is the surface oil. It represents the non-encapsulated oil fraction in contact with pro-oxidant agents present in the environment. It is acknowledged that high percentage of superficial oil triggers lipid oxidation (Menim *et al.*, 2018). It is noteworthy that superficial oil percentage of SA beads is higher in comparison to SA-NM hydrogel beads (Table 1). A possible explanation for this phenomenon lies in the different transport of water molecules during the evaporation in the drying process that might affect the structure of the beads. The higher superficial oil shown by SA samples might be due to the higher porosity resulting from fast water evaporation on the surface, facilitating the migration of the oil molecules from the interior to the surface of the beads. In addition, these results infer that the pore size distribution of SA beads are larger than that of SA-NM hydrogel beads, facilitating the diffusion of oil from the inside of the beads to their surface. The conformation of the pores in the structure of the beads is going to be dependent on the drying process during the dehydration of the hydrogels, the selection of the wall materials and their compositions in the process of encapsulation by ionic gelation.

On the other hand, the SA-NM hydrogel beads displayed encapsulation efficiency between 75.44% to SA-NM (1:1) and 80.64% to SA-NM (1:1.5). These values turned out to be higher than that of the SA beads, which presented a value of 63.48%. The high encapsulation efficiency values can be attributed to the high oil retention capacity of the NM that has

a high protein content (approximately 6.4%) that is the nonpolar part to which is attributed the interaction with oil (Rivera-Corona *et al.*, 2014). The higher oil holding capacity is related to the presence of nonpolar chains of the protein residues in the biopolymer as well as its conformational features that allow them to bind to hydrocarbon units of sesame oil. Menin *et al.* (2018) also reported high encapsulation efficiency for flaxseed oil encapsulated in pectin beads.

Table 1 shows the payload percentages of the different systems studied. The payload is a parameter that depends on the extraction capacity of the oil, that is, it is a measure of the weight of sesame oil that is capable of containing a bead, based on the amount of biopolymer used. As can be seen, the payload of the SA beads presented a very low value compared to the SA-NM hydrogels beads. This can be explained by the fact that the drying process of the SA beads by forced convection modified their microstructure, being less robust and highly porous, favoring the release of the extracted oil. On the other hand, the microstructure of the SA-NM hydrogel beads after drying apparently was more complex due to the interaction that took place between the biopolymers, delaying the release of sesame oil from its interior. In fact, it is known that depending on the type of drying that is used in the dehydration of the beads, many of its structural characteristics can be affected (Garti & McClements, 2012). Menin *et al.* (2018) exhibited higher payloads (> 68%) when they used fluidized bed drying for the dehydration of linseed oil beads with pectin as shell material.

3.3 Lipid oxidation

Figure 2 shows the oxidation kinetics of free SO, SA beads and SA-NM hydrogel beads stored eight weeks (under dark conditions) at 25, 35 and 45 °C and water activities of 0.329, 0.318 and 0.313, respectively. For all temperatures, the stability of the peroxide value (PV) for free oil was higher than for beads. At week 0, free SO presented low PV between 5.03 ± 0.03 and 5.59 ± 0.05 meq HP/kg oil, while the encapsulated SO ranging from 3.14 ± 0.40 to 4.01 ± 0.22 meq HP/kg oil. The values for free and encapsulated oil were similar with no significant differences ($p > 0.05$) between different systems. In this way, the results indicated that the encapsulation process did not exert a negative impact on the oxidative degradation of sesame oil. In addition, the oxidative stability of a vegetable oil is dependent of the antioxidant amount of the raw material quality and of the conditions of

processing and storage; the sesame oil is considered an oil with high presence of natural antioxidant as tocopherols, sesamol and others lignans (Corso *et al.*, 2010).

At six weeks and at any storage temperature, the free SO differed expressively from the encapsulated SO with peroxide values peaks (maximum HP concentration) between 26.30 ± 0.15 meq HP/kg oil and 29.68 ± 0.10 meq HP/kg oil. The SA beads showed variations between 20 ± 0.50 and 21.3 ± 0.28 meq HP/kg oil. The SA-NM hydrogel beads (1:1 w/w) reached to maximum PV values between 9.56 ± 0.08 and 17.1 ± 0.02 meq HP/kg oil, and the SA-NM hydrogel beads (1:1.5 w/w) had PV values between 6.60 ± 0.10 and 15.1 ± 0.16 meq HP/kg oil. At longer storage times, the peroxide value decreased continuously because the hydroperoxides reacted to form secondary lipid oxidation products (carbonyls and aldehydes) (Timilsena *et al.*, 2016).

On the other hand, regardless of storage temperature, the thermal influence on PV stability is observed in Fig. 2. It can be seen that higher temperatures boost the formation of peroxides, either, due to the initiation, propagation step and the decomposition of hydroperoxyl radicals. The oxidative reactions involving PUFAs lead to unacceptable sensory issues for consumers, loss in nutritional value and may sometime cause health disorders (Alpizar-Reyes *et al.*, 2020).

Regarding the effect of storage time, the maximum peroxide value that sesame oil can reach for human consumption according to the CODEX Alimentarius Commission should be less than 10 mEq / kg of oil (Stan, 1999). The maximum peroxide value for free SO was achieved at first week of storage, independently of storage temperature. When SO was encapsulated using SA, the limit peroxide value was reached in the first week at any storage temperature. The greatest effect of protection against oxidation of SO was reached with the mixtures SA-NM as wall materials. As the proportion of NM increases in the mixtures, the protective effect increases, whose permissible limit peroxide values, were found until the sixth week for hydrogels beads SA-NM (1:1) at 25 °C and between the third and fourth week for the beads stored at 35 and 45 °C. In the case of SA-NM hydrogel beads (1:1.5) stored at 25 °C, the maximum peroxide value for human consumption was not reached, while for beads at 35 °C it was reached in the sixth week and for beads at 45 °C it was reached at the fourth week.

The protective effect that NM provides to sesame oil in hydrogels can be explained by the fact that NM modifies the structure of the gel and reduces

its porosity. This fact is possibly due to the strong electrostatic interaction that occurs between the NM and the SA during the ionic gelation process, promoting the formation of a robust complex on the surface of the hydrogel beads. In addition, NM is composed of antioxidants capable to scavenge free radicals, highlighting a high concentration of ascorbic acid, among other compounds, which retard the oxidation.

3.4 Oxidation kinetics of free and encapsulated SO

An integral method was used for determining the reaction order of hydroperoxides (HP) formation by oxidation of free and encapsulated SO. The experimental data (Figure 2) were fitted to equations (5)-(7). All systems showed a better fit to zero-order kinetics ($r^2 \geq 0.950$) until reaching their maximum HP concentration over the time. This means that the rate of hydroperoxides formation is not concentration dependent, and only depends on thermal effects. Peroxide values were plotted as function of storage time to obtain the apparent reaction rate constants of hydroperoxide formation for both free oil and encapsulated SO (K_{HP}). Table 2 summarize the calculated kinetic parameters of the free oil and encapsulated SO oxidation. As can be observed, the apparent reaction rate constants (K_{HP}) values increased as temperature increased at a specific water activity, independently of the storage temperature. The reaction rate constants of non-encapsulated SO were significantly ($p \leq 0.05$) higher than that of SA beads and both of them were significantly higher (approximately 2.3-6.5 fold times) than (K_{HP}) of SO hydrogel beads coating with SA-NM (1:1 w/w) and SA-NM (1: 1.5 w/w) mixtures. Greater rate constants of HP formation (K_{HP}) values indicate a higher oxygen diffusion in free SO, whilst oxygen diffusion was retarded through the biopolymer matrix of the wall materials of the SO hydrogel beads, indicating that as the proportion of NM in the mixtures increases, the SA-NM hydrogel beads achieve the greatest protection of SO against oxidation.

The values of the apparent activation energy for all the systems studied were calculated according to equation 8 ($r^2 \geq 0.94$). The value of the apparent activation energy (E_a) of the free oil was 3.49 ± 1.13 kJ/mol, the value of (E_a) of SA beads was 3.09 ± 1.02 kJ/mol, and the values of the (E_a) SA-NM hydrogels beads (1: 1) and (1: 1.5) were 24.29 ± 1.05 and

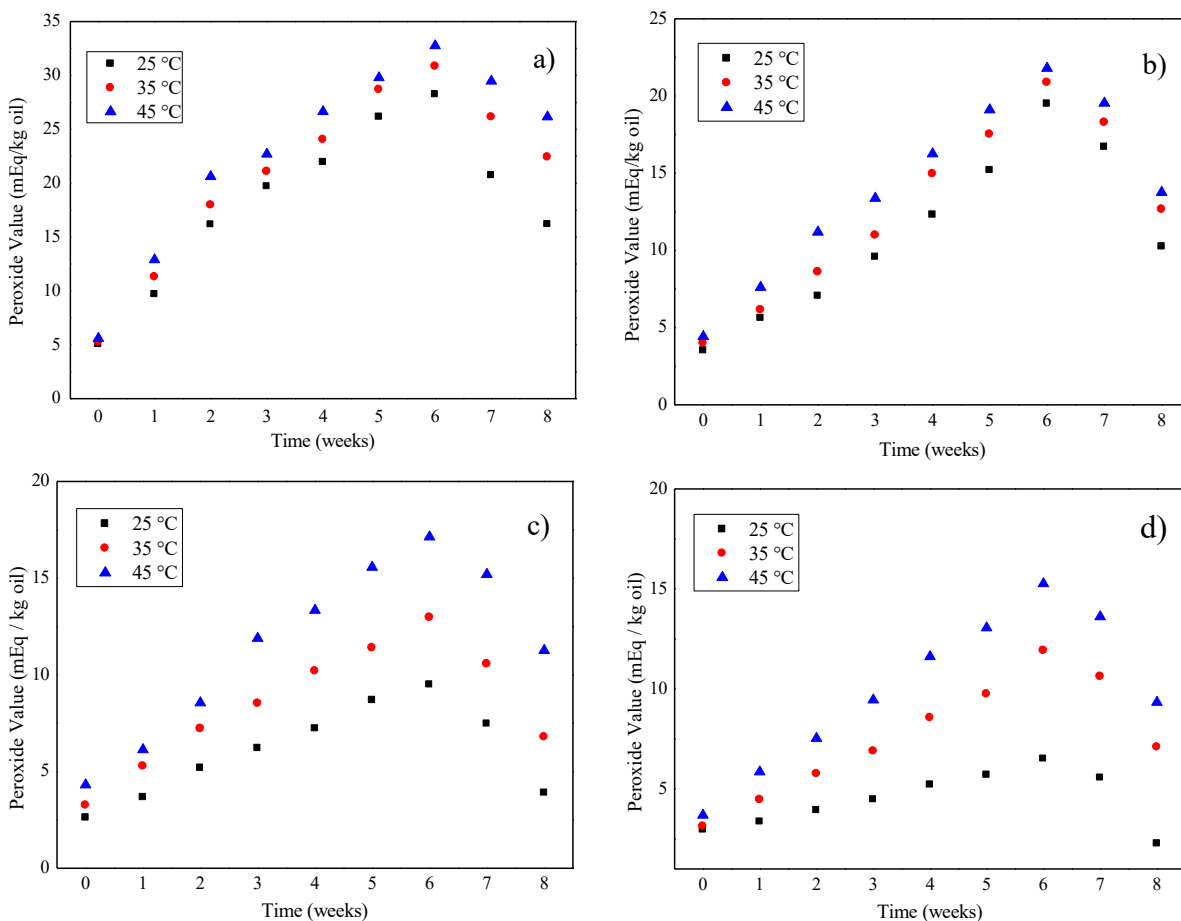


Figure 2. Lipid oxidation of: a) free sesame oil (SO); b) SA; c) SA-NM (1:1) and d) SA-NM (1:1.5) hydrogel beads, stored during eight weeks, at 25, 35 and 45 °C. Average values are shown ($n=3$).

45.04±1.01 kJ/mol, respectively. In accordance with the activation energy concept, SA-NM hydrogel beads have the highest E_a values, which means that more energy is required for the oxidation reaction of the oil to begin within the matrix (Fogler, 2006). On the other hand, practically the same energy is required for the formation of peroxides in the free sesame oil and in the SA beads. The calculated values of activation energy for the hydrogel beads SO suggest that oxidation was an oxygen diffusion-controlled process.

3.5 Release kinetics of sesame oil extracted in hydrogel beads systems

Figure 3 shows the sesame oil extraction profiles of SA, SA-NM (1:1 w/w) and SA-NM (1:1.5 w/w) hydrogel beads in a non-polar solvent subjected to different stirring times. The oil release was evaluated

by successive extractions of the oil with n-hexane after stirring. The oil migrated much faster from the inner of the bead to the surface in SA than in SA-NM (1:1 w/w) and SA-NM (1:1.5 w/w) beads, indicating that the addition of nopal mucilage enhanced the lipid retention. In all systems, the release mechanism of SO from the hydrogel beads was matrix diffusion-controlled, this was evidenced by the apparent activation energy values obtained in the lipid oxidation study of the beads. When the transport mechanism is controlled only by diffusion, it is related to the structural characteristics of the wall materials that forming the matrix of the beads (Chan, 2011).

It has been reported that the internal structure of beads formed only with sodium alginate as wall material in the encapsulation of oils is extremely porous, with relatively large pore sizes (Bannikova *et al.*, 2018; Menin *et al.*, 2018).

Table 2. Zero-order kinetic parameters of free SO and SO hydrogel beads.

T = 25 °C			
	Kinetic model $C_{HP} = K_{HP}t + C_{HP_0}$	K_{HP} (meq hydroperoxides/ kg of oil • week)	r^2
Free SO	$C_{HP} = 3.869t + 6.528$	3.869 ± 0.15^a	0.974
SA	$C_{HP} = 2.584t + 2.642$	2.584 ± 0.09^b	0.976
SA-NM (1:1)	$C_{HP} = 1.167t + 2.653$	1.167 ± 0.24^c	0.996
SA-NM (1:1.5)	$C_{HP} = 0.595t + 2.807$	0.595 ± 0.14^d	0.993
T = 35 °C			
	Kinetic model $C_{HP} = K_{HP}t + C_{HP_0}$	K_{HP} (meq hydroperoxides/ kg of oil • week)	r^2
Free SO	$C_{HP} = 4.205t + 7.268$	4.205 ± 0.38^a	0.973
SA	$C_{HP} = 2.848t + 3.326$	2.848 ± 0.25^b	0.993
SA-NM (1:1)	$C_{HP} = 1.585t + 3.652$	1.585 ± 0.32^c	0.994
SA-NM (1:1.5)	$C_{HP} = 1.418t + 2.958$	1.418 ± 0.24^d	0.992
T = 45 °C			
	Kinetic model $C_{HP} = K_{HP}t + C_{HP_0}$	K_{HP} (meq hydroperoxides/ kg of oil • week)	r^2
Free SO	$C_{HP} = 4.333t + 8.571$	4.333 ± 0.28^a	0.954
SA	$C_{HP} = 2.864t + 4.008$	2.864 ± 0.15^b	0.997
SA-NM (1:1)	$C_{HP} = 2.218t + 4.333$	2.218 ± 0.39^b	0.990
SA-NM (1:1.5)	$C_{HP} = 1.900t + 3.794$	1.900 ± 0.41^b	0.998

Data are presented as means \pm SD (n = 3).

Values with different letters in the same column indicate significant difference ($p \leq 0.05$).

Free SO: free sesame oil; SA: sodium alginate; NM: nopal mucilage; C_{HP_0} : initial peroxide value at time (t) zero; C_{HP} : peroxide value after time (t); K_{HP} : hydroperoxides formation rate constant; r^2 : coefficient of linear determination.

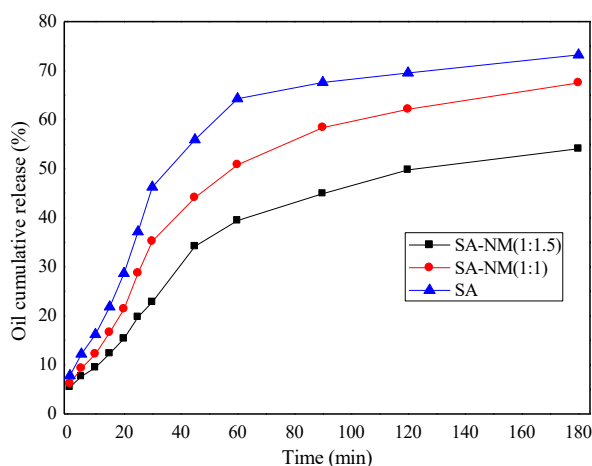


Figure 3. Cumulative release profiles of SA and SA - NM hydrogel beads at 25 °C. Average values are shown (n=3). SA: sodium alginate; NM: nopal mucilage.

These structural characteristics promote faster oil extraction, which was demonstrated in its release profile that was higher compared to the profiles of SA-NM mixtures. In the case of the SA-NM hydrogel beads, the oil molecules were trapped in the matrix of these biopolymers because a high tortuosity was

formed in their internal structure, as result of a complex formation between the SA and the NM. Furthermore, as the amount of NM in the mixtures increased, oil release rate was slower. These results clearly indicate that NM exerted higher oil retention in the inner structure of the beads.

Conclusions

This study provides a new way for preventing the oxidation of sesame oil by ionic gelation method, where SO can be encapsulated in sodium alginate-nopal mucilage hydrogel beads as wall material. The SA-NM hydrogel beads had heterogeneous surface morphologies, where el NM acted as structural support and controlling fractures in the beads after drying process, making the gel matrix more flexible. SA-NM hydrogel beads after the drying process leads to an irregular spherical shape that the SA beads. SA-NM hydrogel beads is characterized by high yield (>83.34%) and encapsulation efficiency (> 75.44%), and limited surface oil (< 6.20%). The greatest effect of protection against oxidation of SO was reached as the proportion of NM increases in the mixtures, due to the strong electrostatic interaction that occurs between the NM and the SA during the ionic gelation process, promoting the formation of a robust complex on the surface of the hydrogel beads. Finally, the ionic gelation method turned out to be a competitive option to encapsulate and protect sesame oil in comparison to most common methods such as spray drying, lyophilization, fluidized bed drying and coacervation. It is an easy to implement technology, does not operate at high or low temperatures that affect the deterioration of the encapsulated agent and does not require pretreatment of the encapsulating agents to be used. However, it does not offer a great diversity of biopolymers as encapsulating agents with respect to those that can be used in other encapsulation technologies. In addition, the particle sizes obtained by ion gelation are significantly larger compared to techniques such as spray drying and complex coacervation, although the size will ultimately depend on the product that needs to be produced and marketed.

Acknowledgements

The authors wish to acknowledge the partial financial support of this research to the Universidad Autónoma del Estado de México through grant 4738/2019/CIB. Besides the authors want to thank the financial support provided to the author S.K. Velázquez-Gutiérrez who received a scholarship with number 481491 through the Consejo Nacional de Ciencia y Tecnología (CONACyT) of Mexico.

References

- Alpizar-Reyes, E., Varela-Guerrero, V., Cruz-Olivares, J., Carrillo-Navas, H., Alvarez-Ramirez, J., & Pérez-Alonso, C. (2020). Microencapsulation of sesame seed oil by tamarind seed mucilage. *International Journal of Biological Macromolecules* 145, 207-215. <https://doi.org/10.1016/j.ijbiomac.2019.12.162>.
- Bannikova, A., Evteev, A., Pankin, K., Evdokimov, I., & Kasapis, S. (2016). Microencapsulation of fish oil with alginate: *In-vitro* evaluation and controlled release. *LWT - Food Science and Technology* 90, 310-315. <https://doi.org/10.1016/j.lwt.2017.12.045>.
- Benavides, S., Cortés, P., Parada, J., & Franco, W. (2016). Development of alginate microspheres containing thyme essential oil using ionic gelation. *Food Chemistry* 204, 77-83. <http://dx.doi.org/10.1016/j.foodchem.2016.02.104>.
- Bligh, E.G., & Dyer, W. J. (1959). A rapid method of total lipid extraction and purification. *Canadian Journal of Biochemistry and Physiology* 37, 911-917.
- Chan, E.S. (2011). Preparation of Ca-alginate beads containing high oil content: Influence of process variables on encapsulation efficiency and bead properties. *Carbohydrate Polymers* 84, 1267-1275. doi: [10.1016/j.jcis.2009.05.027](https://doi.org/10.1016/j.jcis.2009.05.027).
- Charoen, R., Jangchud, A., Jangchud, K., Harnsilawat, T., & McClements, D.J. (2015). The physical characterization and sorption isotherm of rice bran oil powders stabilized by food-grade biopolymers. *Drying Technology* 33, 479-492. <https://www.tandfonline.com/doi/abs/10.1080/07373937.2014.962142>.
- Chen, L. Y., Remondetto, G. E., & Subirade, M. (2006). Food protein-based materials as nutraceutical delivery systems. *Trends in Food Science & Technology* 17, 272-283. doi: [10.1016/j.tifs.2005.12.011](https://doi.org/10.1016/j.tifs.2005.12.011).
- Corso, M.P., Fagundes-Klena, M.R., Silva, E.A., Filho, L.C., Santos, J.N., Freitas, L.S., & Dariva,

- C. (2010). Extraction of sesame seed (*Sesamum indicum* L.) oil using compressed propane and supercritical carbon dioxide. *The Journal of Supercritical Fluids* 52, 56-61. doi: [10.1016/j.supflu.2009.11.012](https://doi.org/10.1016/j.supflu.2009.11.012).
- Cortés-Camargo, S., Gallardo-Rivera, R., Barragán-Huerta, B.E., Dublán-García, O., Román-Guerrero, A., & Pérez-Alonso, C. (2018). Exploring the potential of mesquite gum-nopal mucilage mixtures: Physicochemical and functional properties. *Journal of Food Science* 83, 113-121. doi: [10.1111/1750-3841.13937](https://doi.org/10.1111/1750-3841.13937).
- Escalona-García, L.A., Pedroza-Islas, R., Natividad, R., Rodríguez-Huezo, M.E., Carrillo-Navas, H., & Pérez-Alonso, C. (2016). Oxidation kinetics and thermodynamic analysis of chia oil microencapsulated in a whey protein concentrate-polysaccharide matrix. *Journal of Food Engineering* 175, 93-103. <http://dx.doi.org/10.1016/j.jfoodeng.2015.12.009>.
- Fogler, H.S. (2006). *Elements of Chemical Reaction Engineering*, fourth ed., pp. 79-142 Upper Saddle River, New Jersey.
- Fuentes-Ortega, T., Martínez-Vargas, S.L., Cortés-Camargo, S., Guadarrama-Lezama, A.Y., Gallardo-Rivera, R., Baeza-Jiménez, R., & Pérez-Alonso, C. (2017). Effects of the process variables of microencapsulation sesame oil (*Sesamum indica* L.) by spray drying. *Revista Mexicana de Ingeniería Química* 16, 477-490. <http://www.rmiq.org/iqfvp/Pdfs/Vol.%2016,%20No.%202/Alim8/RMIQTemplate.pdf>.
- Garti, N., & McClements, D. J. (2012). *Encapsulation Technologies and Delivery Systems for Food Ingredients and Nutraceuticals*. Philadelphia: Woodhead Publishing Limited.
- Hernández-Centeno, F., Hernández-González, M., López-De la Peña, H.Y., López-Trujillo, R., Zamudio-Flores, P.B., Ochoa-Reyes, E., Tirado-Gallegos, J.M., & Martínez-Vázquez, D.G. (2020). Changes in oxidative stability, composition and physical characteristics of oil from a non-conventional source before and after processing. *Revista Mexicana de Ingeniería Química* 19, 1389-1400. <https://doi.org/10.24275/rmiq/Alim937>.
- Hosseini S.M., Hosseini, H., Mohammadifar, M.A., Mortazavian, A.M., Mohammadi, A., Khosravi-Darani, K., Shojaee-Aliabadi, S., Dehghan, S., & Khaksar, R. (2013). Incorporation of essential oil in alginate microparticles by multiple emulsion/ionic gelation. *International Journal of Biological Macromolecules* 62, 582-588. <http://dx.doi.org/10.1016/j.ijbiomac.2013.09.054>.
- Joye, I. J., & McClements, D. J. (2014). Biopolymer-based nanoparticles and microparticles: fabrication, characterization, and application. *Current Opinion in Colloid & Interface Science* 19, 417-427. <http://dx.doi.org/10.1016/j.cocis.2014.07.002>.
- Lee, E., & Choe, E. (2012). Changes in oxidation-derived off-flavor compounds of roasted sesame oil during accelerated storage in the dark. *Biocatalysis and Agricultural Biotechnology* 1, 89-93. doi: [10.1016/j.bcab.2011.08.003](https://doi.org/10.1016/j.bcab.2011.08.003).
- León-Martínez, F.M., Méndez-Lagunas, L.L., & Rodríguez-Ramírez, J. (2010). Spray drying of nopal mucilage (*Opuntia ficus-indica*): Effects on powder properties and characterization. *Carbohydrate Polymers* 81, 864-70. doi: [10.1016/j.carbpol.2010.03.061](https://doi.org/10.1016/j.carbpol.2010.03.061).
- Levenspiel, O. (1999). *Chemical Reaction Engineering*, third ed., pp. 38-82 New York
- Li, Y., Hu, M., Du, Y., Xiao, H., & McClements, D. J. (2011). Control of lipase digestibility of emulsified lipids by encapsulation within calcium alginate beads. *Food Hydrocolloids* 25, 122-130. doi: [10.1016/j.foodhyd.2010.06.00](https://doi.org/10.1016/j.foodhyd.2010.06.00).
- Martín, A., Varona, S., Navarrete, A., & Cocero, M. J. (2010). Encapsulation and coprecipitation processes with supercritical fluids: Applications with essential oils. *Open Chemical Engineering* 4, 31-41. <https://benthamopen.com/DOWNLOAD-PDF/TOCENGJ-4-31>.
- Medina-Torres, L., Brito-De La Fuente, E., Torrestiana-Sanchez, B., & Alonso, S. (2003). Mechanical properties of gels formed by mixtures of mucilage gum (*Opuntia ficus indica*) and carrageenans. *Carbohydrate*

- Polymers* 52, 143-150. [https://doi.org/10.1016/S0144-8617\(02\)00269-2](https://doi.org/10.1016/S0144-8617(02)00269-2).
- Medina-Torres, L., García-Cruz, E.E., Calderas, F., González-Laredo, R.F., Sánchez-Olivares, G., Gallegos-Infante, J.A., Rocha-Guzmán, N.E., & Rodríguez-Ramírez, J. (2013). Microencapsulation by spray drying of gallic acid with nopal mucilage (*Opuntia ficus indica*). *LWT - Food Science & Technology* 50, 642-650. <http://dx.doi.org/10.1016/j.lwt.2012.07.038>.
- Menin, A., Zanoni, F., Vakarelova, M., Chignola, R., Donà, G., Rizzi, C., Mainente, F., & Zoccatelli, G. (2018). Effects of microencapsulation by ionic gelation on the oxidative stability of flaxseed oil. *Food Chemistry* 219, 293-299. <https://doi.org/10.1016/j.foodchem.2018.06.144>.
- Moreno-Santander, C., García-Zapateiro, L.A., & Ortega-Toro, R. (2020). Rheological characterization of gums-gel obtained from the proteic isolate of sesame (*Sesamum indicum*). *Revista Mexicana de Ingeniería Química* 19, 21-31. <https://doi.org/10.24275/rmiq/Alim581>.
- Pereyra-Castro, S.C., Pérez-Pérez, V., Hernández-Sánchez, H., Jiménez-Aparicio, A., Gutiérrez-López, G.F., & Alamilla-Beltrán, L. (2019). Effect of composition and homogenization pressure of chia oil emulsions elaborated by microfluidization. *Revista Mexicana de Ingeniería Química* 18, 69-81. <https://doi.org/10.24275/uam/izt/dcbi/revmexingquim/2019v18n1/Pereyra>.
- Plazola-Jacinto, C.P., Pérez-Pérez, V., Pereyra-Castro, S.C., Alamilla-Beltrán, L., & Ortiz-Moreno, A. (2019). Microencapsulation of biocompounds from avocado leaves oily extracts. *Revista Mexicana de Ingeniería Química* 20, 1261-1276. <https://doi.org/10.24275/uam/izt/dcbi/revmexingquim/2019v18n3/Plazola>.
- Pu, J., & Sathivel, S. (2011). Kinetics of lipid oxidation and degradation of flaxseed oil containing crawfish (*Procambarus clarkia*) astaxanthin. *Journal of the American Oil Chemists' Society* 88, 595-601. <https://doi.org/10.1007/s11746-010-1713-8>.
- Ramos, P.E., Silva, P., Alario, M.M., Pastrana, L.M., Teixeira, J.A., Cerqueira, M.A., & Vicente, A.A. (2018). Effect of alginate molecular weight and M/G ratio in beads properties foreseeing the protection of probiotics. *Food Hydrocolloids* 77, 8-16. <http://dx.doi.org/10.1016/j.foodhyd.2017.08.031>.
- Rivera-Corona, J.L., Rodríguez-González, F., Rendón-Villalobos, R., García-Hernández, E., & Solorza-Feria, J. (2014). Thermal, structural and rheological properties of sorghum starch with cactus mucilage addition. *LWT - Food Science & Technology* 59, 806-12. <http://dx.doi.org/10.1016/j.lwt.2014.06.011>.
- Rodea-González, D.A., Cruz-Olivares, J.C., Román-Guerrero, A., Rodríguez-Huezo, M.E., Vernon-Carter, E.J., & Pérez-Alonso, C. (2012). Spray-dried encapsulation of chia essential oil (*Salvia hispanica* L.) in whey protein concentrate-polysaccharide matrices. *Journal of Food Engineering* 111, 102-109. doi: 10.1016/j.jfoodeng.2012.01.020.
- Sáenz, C., Sepúlveda, E., & Matsuhira, B. (2004). *Opuntia* spp. mucilage? s: a functional component with industrial perspectives. *Journal of Arid Environments* 57, 275-90. doi: 10.1016/S0140-1963(03)00106-X.
- Shahidi, F., & Zhong, Y. (2005). Lipid oxidation: Measurement methods. *Bailey's Industrial Oil and Fat Products*. John Wiley & Sons, Inc. <https://onlinelibrary.wiley.com/doi/abs/10.1002/047167849X.bio050>.
- Shantha, N.C., & Decker, E.A. (1994). Rapid, sensitive, iron-based spectrophotometric method for determination of peroxide values of food lipids. *Journal of AOAC International* 77, 421-424. <https://doi.org/10.1093/jaoac/77.2.421>.
- Shewan, H. M., & Stokes, J. R. (2013). Review of techniques to manufacture micro hydrogel particles for the food industry and their applications. *Journal of Food Engineering* 119, 781-792. <http://dx.doi.org/10.1016/j.jfoodeng.2013.06.046>.
- Stan, C. (1999). *Codex Alimentarius Standard for Edible Fats and Oils*, pp. 2-7.

- Timilsena, Y. P., Adhikari, R., Barrow, C. J., & Adhikari, B. (2016). Microencapsulation of chia seed oil using chia seed protein isolate-chia seed gum complex coacervates. *International Journal of Biological Macromolecules*, 91, 347-357. <https://doi.org/10.1016/j.ijbiomac.2016.05.058>.
- Timilsena, Y.P., Akanbi, T.O., Khalid, N., Adhikari, B., & Barrow, C.J. (2019). Complex coacervation: Principles, mechanisms and applications in microencapsulation. *International Journal of Biological Macromolecules* 121, 1276-1286. <https://doi.org/10.1016/j.ijbiomac.2018.10.144>.
- Vasile, F.M., Romero, A.M., Judis, M.A., & Mazzobre, M.F. (2016). *Prosopis alba* exudate gum as excipient for improving fish oil stability in alginate-chitosan beads. *Food Chemistry* 190, 1093-1101. <http://dx.doi.org/10.1016/j.foodchem.2015.06.071>.
- Xu-Yan, D., Ping-Ping, L., Fang, W., Mu-lan, J., Ying-Zhong, Z., Guang-Ming, L., Hong, C., & Yuan-Di, Z. (2012). The impact of processing on the profile of volatile compounds in sesame oil. *European Journal of Lipid Science and Technology* 114, 277-286. doi: [10.1002/ejlt.201100059](https://doi.org/10.1002/ejlt.201100059).